Enhanced Photoluminescence Properties of Li/Al-doped YPO_4:Eu Phosphors

R. Balakrishnaiah[a,b], Dong Woo Kim[a], Soung Soo Yi[a,*], Sung Hoon Kim[c] , Kiwan Jang[d], Ho Sueb Lee[d], Byung Kee Moon[b] and Jung Hyun Jeong[b]

[a]Department of Electronic Materials Engineering, Silla University, Busan 617-736, Republic of Korea
[b]Department of Physics, Pukyong National University, Busan 608-737, Republic of Korea
[c]Department of Engineering in Energy and Applied Chemistry, Silla University, Busan 617-736, Republic of Korea
[d]Department of Physics, Changwon National University, Changwon 641-773, Republic of Korea
([*]Corresponding author, e-mail: ssyi@silla.ac.kr)

ABSTRACT

Different concentrations of Li/Al-doped YPO_4:$Eu_{0.05}$ phosphors have been prepared by the solid state reaction method and are characterized by X-ray diffraction, scanning electron microscopy, excitation and emission measurements. The dependence of various optical and morphological properties of the prepared materials on Li/Al concentration has been discussed in our present work. Incorporation of Li^+/Al^{3+} ions into the YPO_4:Eu phosphors has greatly enhanced the crystallinity, particle size and hence the luminescence properties and the optimum concentration in case of both Li and Al dopants are found to be 10 mol %. The improvement in PL performance with Li/Al-doping may result from the improved crystallinity and from the enlarged grain sizes inducing lower scattering loss and distortion of symmetry. The results are discussed in comparison of results with similar reported works.

Keywords: Photoluminescence, Lanthanide-doped phosphors, X-ray diffraction, Lithium

1 INTRODUCTION

Research interest on lanthanide (Ln)-doped materials is one of the fascinating field among the present scientific community due to their potential applications in the development of plasma display panels (PDPs), field emission displays (FEDs), Cathode ray tubes (CRTs) and electro-luminescent devices (ELDs). Recently, $LnPO_4$ (Ln = Y, La, Gd, Lu) materials have attracted much attention in PDP applications due to their high thermal and chemical stability and high luminescence efficiency under VUV excitation. Among activator ions, Eu^{3+} ion is one of the most interesting ions due to its simple lower energy levels scheme as well as applications in the fields such as red emitting phosphor by its intense, narrow and monochromatic red emission around 610 nm as a result of $^5D_0 \rightarrow {}^7F_2$ transition [1-3]. Therefore YPO_4:Eu phosphors are found to be one of the most familiar red emitting phosphors. However, in YPO_4:Eu phosphors, the intensity of red emission, which occurs at 610 nm in these phosphors, is lower than that of orange emission that occurs at 593 nm, leading to a poor chromaticity. It is thus necessary either to improve the luminescence properties of these already existing phosphors or to develop new phosphors. Since the red emission coming from the $^5D_0 \rightarrow {}^7F_2$ transition is hypersensitive to the lattice symmetry of the host crystal, it is possible to tune the intensity of red emission by modifying the neighboring network design around Eu^{3+} ions on introducing other atoms such as Ca, Sr, Ba, Zn, Al, Li, Sc, Bi, La, Gd, etc. into the host matrices. Therefore, much effort is being made on the control of symmetry, morphology and structure of these materials to obtain desirable luminescence properties. It is observed from literature that incorporation of metal ions having smaller ionic radius have more effect in improving the luminescence properties. Substitution of Li^+ ions in to the Y^{3+} sites creates the oxygen vacancies and these oxygen vacancies play a vital role in determining the morphology and energy transfer rates and hence improves the emission intensity. It is well known that incorporation of Al^{3+} ions also plays an important role in improving the luminescence as well as mechanical properties of materials [1-8].

2 EXPERIMENTAL

The $Y_{(0.95-x)}Eu_{0.05}PO_4$:$Li_{(x)}$/$Al^{3+}{}_{(x)}$ (x = 0.00, 0.05, 0.10, 0.15 and 0.20 mol) powder phosphors are synthesized by the conventional solid state reaction method under ambient pressure in a tubular electric furnace using high purity chemicals of Y_2O_3, P_2O_5, Eu_2O_3, Li_2CO_3 and Al_2O_3. The stoichiometric amounts of chemicals are finely grinded in an agate mortar with pestle adding a little amount of distilled water or acetone. Then the sample is taken in an alumina crucible, sintered at 120 ℃ (3 hr), 1000-1200 ℃ (3 hr) and then annealed at 400 ℃ (10 hr) after which they are allowed to cool down to room temperature. The crystal purity of the prepared samples is examined by XRD analysis using a high-resolution X-ray diffraction system with CuKα1 radiation (λ = 1.542 Å). The surface morphologies of the samples are investigated by a SEM FESEM images collected from field emission gun scanning electron microscope (Quanta 200 FEG) operated at 10-20 kV. The photoluminescence excitation spectra are measured at 594 nm emission peak and the emission spectra are

measured under the 232 and 394 nm excitation wavelengths using xenon lamp as the light source.

3 RESULTS AND DISCUSSION

3.1 Li^+-doped YPO_4:Eu phosphors

The XRD patterns of the $Y_{(0.95-x)}Eu_{0.05}PO_4:Li^+_{(x)}$ samples along with theoretical data for YPO_4 (JCPDS No. 09-0377) are shown in Fig. 1. As can be seen from Fig. 1, the observed diffraction peaks well-matched with the theoretical data of YPO_4 indicating the successful formation of xenotime type tetragonal phase structure of YPO_4 samples. It indicates that Eu^{3+} and Li^+ ions are substituted into the Y^{3+} sites without formation of any additional phase. The crystallinity of the samples is found much improved with Li^+-doping. The surface morphologies of the Li-doped

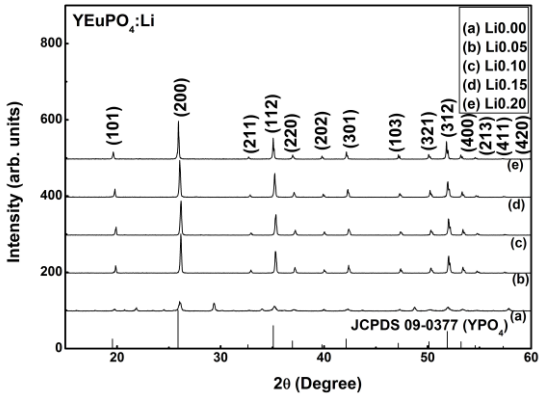

Figure 1: XRD patterns of $Y_{(0.95-x)}Eu_{0.05}PO_4:Li_{(x)}$ phosphors for x = (a) 0.00, (b) 0.05, (c) 0.10, (d) 0.15 and (e) 0.20 mol concentration of Al^{3+} ions along with JCPDS data for YPO_4 (09-0377).

YPO_4:Eu phosphors as a function of Li^+ ion concentration are shown in Fig. 2 which shows solid microcrystalline particles for of the phosphors. The shapes and sizes of the particles in the Li-doped phosphors can be found improved when compared to that of undoped phosphor.

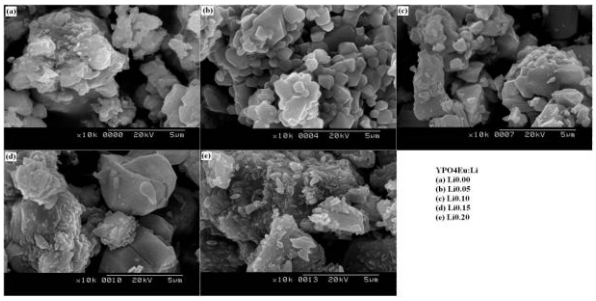

Figure 2: SEM images of $Y_{(0.95-x)}Eu_{0.05}PO_4:Li_{(x)}$ phosphors for x = (a) 0.00, (b) 0.05, (c) 0.10, (d) 0.15 and (e) 0.20 mol concentration of Li^+ ions.

3.2 Al^{3+}-doped YPO_4:Eu phosphors

The XRD patterns of the $Y_{(0.95-x)}Eu_{0.05}PO_4:Al^{3+}_{(x)}$ samples along with theoretical data for YPO_4 (JCPDS No. 09-0377) are shown in Fig. 3. As can be seen from Fig. 3, the observed diffraction peaks well-matched with the theoretical data of YPO_4 indicating the successful formation

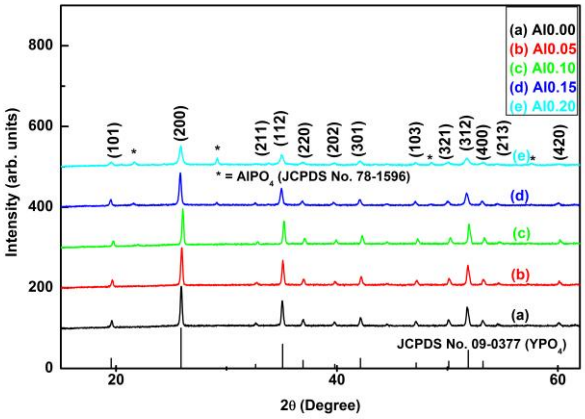

Figure 3: XRD patterns of $Y_{(0.95-x)}Eu_{0.05}PO_4:Al_{(x)}$ phosphors for x = (a) 0.00, (b) 0.05, (c) 0.10, (d) 0.15 and (e) 0.20 mol concentration of Al^{3+} ions along with JCPDS data for YPO_4 (09-0377).

of xenotime type tetragonal phase structure of YPO_4 samples. It indicates that Eu^{3+} and Al^{3+} ions are substituted into the Y^{3+} sites without formation of any additional phase at lower concentrations. However, for Al^{3+} ion concentrations beyond 0.10 mol, additional hexagonal peaks relating to $AlPO_4$ phase (JCPDS No. 78-1596) with larger lattice constants a = 13.77 and c = 8.378 Å are observed at 2θ of around 21.56, 29.14, 48.50 and 57.54 degrees (represented by '*' mark). The crystallinity of the samples is found slightly improved with increase in concentration of Al^{3+} ions from 0.00 to 0.10 mol and then decreased for higher concentrations associated with increase in $AlPO_4$ phase. The crystallite size in (200) direction was calculated for all the samples using the Debye-Scherrer formula [9] and are found to be 408, 408, 480, 371 and 272 Å for 0.00, 0.05, 0.10, 0.15 and 0.20 mol concentrations of Al^{3+} ions, respectively. The diffraction peak positions as a function of Al^{3+} ion concentration are shown in Fig. 4(a). As can be noticed, the peak positions are slightly shifted towards higher angle direction with increase in concentration of Al^{3+} ions from 0.00 mol to 0.10 mol which might be attributed to lattice contraction because of substitution of larger sized Y^{3+} ion (ionic radius = 90 pm) sites by the smaller sized Al^{3+} ions (ionic radius = 54 pm) in the $Y_{(0.95-x)}Eu_{0.05}PO_4$ phosphors. The lattice parameters a and c for the tetragonal structure along with c/a values have been calculated for all the Al^{3+}-doped

YPO_4:Eu^{3+} samples and are shown in Fig. 4(b) as a function of Al^{3+} ion concentration. The theoretical values of a, c and

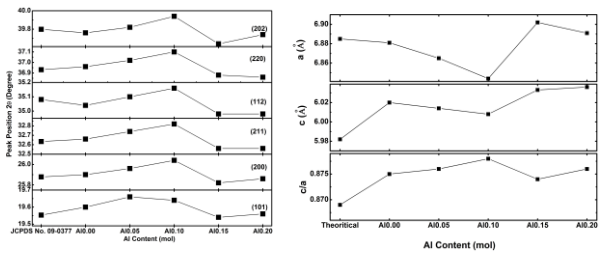

Figure 4: Variation of (a) diffraction peak positions and (b) lattice parameters a, c and c/a as a function of Al^{3+} ion concentration in $Y_{(0.95-x)}Eu_{0.05}PO_4$:$Al_{(x)}$ phosphors.

c/a are also presented in Fig. 4(b) for comparison. As can be seen from Fig. 4(b), the lattice parameters decreased with increase in concentration of Al^{3+} ions from 0.00 to 0.10 mol and then they are found larger and almost constant for higher concentrations which might be due to formation of additional hexagonal $AlPO_4$ phase with larger lattice parameters. The experimental c/a values are found almost constant (0.875±0.003). Besides, as can be seen from the FESEM images shown in Fig. 5, enhanced grain sizes can be observed for 0.10 mol concentration of Al^{3+} ions.

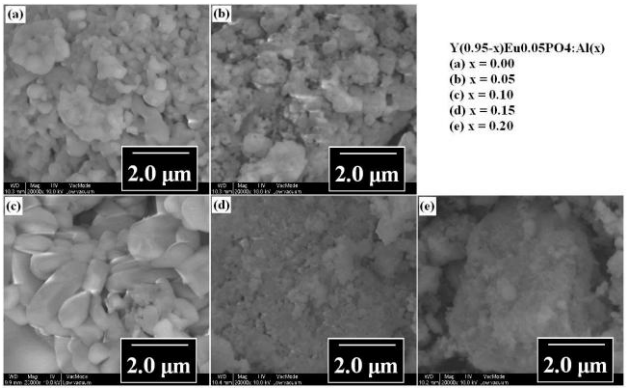

Figure 5: FESEM images of $Y_{(0.95-x)}Eu_{0.05}PO_4$:$Al_{(x)}$ phosphors for x = (a) 0.00, (b) 0.05, (c) 0.10, (d) 0.15 and (e) 0.20 mol concentration of Al^{3+} ions.

The photoluminescence excitation (PLE) (a), as well as emission (PL) spectra (b and c), for various concentrations of Li^+/Al^{3+}-doped $Y_{(0.95-x)}Eu_{0.05}PO_4$ phosphors have also been measured and that of undoped and 0.10 mol Li^+/ Al^{3+}-doped $Y_{(0.95-x)}Eu_{0.05}PO_4$ phosphors is shown in Fig. 6. As can be seen from Fig. 6(a), an intense and broad UV excitation band is observed at 232 nm which can be assigned to the charge transfer band (CTB) of Eu^{3+} - O^{2-} resulting from an electron transfer from the ligand O^{2-} ($2p^6$) orbitals to the empty $4f^6$ states of Eu^{3+} configuration [10, 11]. Another sharp and intense excitation band observed at 394 nm can be assigned to the f-f transitions of Eu^{3+} ions. As can be seen from the emission spectrum shown in Fig. 6 (b and c), an intense emission band is observed at 594 nm under 232 and 394 nm excitation wavelengths which can be assigned to the $^5D_0 \rightarrow {}^7F_1$

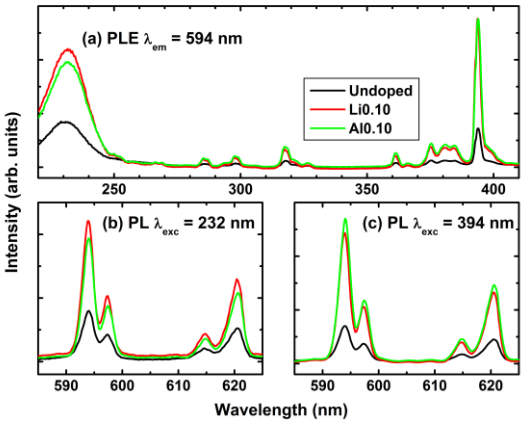

Figure 6: Photoluminescence excitation spectrum (PLE) under (a) 594 nm emission and emission spectrum (PL) under (b) 232 nm and (c) 394 nm excitation in case of undoped and 0.10 mol Li/Al-doped YPO_4:$Eu_{0.05}$ phosphor.

magnetic dipole transition of Eu^{3+} ions while the other emission band observed at 619 nm can be assigned to the $^5D_0 \rightarrow {}^7F_2$ induced electric dipole transition, which is hypersensitive to the local environment around Eu^{3+} ions. The PL intensity increased with increase in concentration of Li^+/Al^{3+} ions from 0.00 to 0.10 mol and the intensity of 0.10 mol Li^+ (Al^{3+})-doped $Y_{(0.95-x)}Eu_{0.05}PO_4$ phosphor was improved by a factor of 2.69 (1.99) under 232 nm excitation while it is found to be 1.25 (1.74) under 394 nm excitation, in comparison with undoped $Y_{(0.95-x)}Eu_{0.05}PO_4$ phosphor. The increase in emission intensity with increase in Li^+/Al^{3+} ion concentration might be attributed to improvement in crystallinity and particle sizes and lowering of symmetry with variations in M/Y ratio (M = Li or Al). In addition, substitution of Li^+ ions into the Y^{3+} sites would naturally relieve a substantial number of oxygen vacancies on the surface of the phosphor. These oxygen vacancies might act as a sensitizer for the energy transfer to Eu^{3+} ion due to the strong mixing of charge transfer states and enhances the luminescence intensity. Besides, further increase of Li^+ content will greatly increase the oxygen vacancies of the host lattice, which will destroy the crystallinity and lead to luminescence quenching as observed when the concentration of Li^+ ions is increased beyond 0.10 mol [12-19].

The red ($^5D_0 \rightarrow {}^7F_2$) to orange ($^5D_0 \rightarrow {}^7F_1$) emission intensity ratio (R/O), also known as asymmetric ratio is also calculated for all the samples and is found improved when the YPO_4:Eu^{3+} phosphors were doped with Li^+/Al^{3+} ions, which might be attributed to lowering of symmetry around

Eu^{3+} ions due to substitution of smaller sized Li^{+}/Al^{3+} ions into the larger sized Y^{3+} ion sites.

The role of Al^{3+} ions in phosphate materials is of much interest, because it not only improves the physical, mechanical, thermal and chemical properties but also affects the fluorescence properties and the most authoritative study of effect of Al^{3+} ions in phosphate structures is given by Brow et al [20, 21]. It is interesting to note that the Al_2O_3 optimum concentration observed in the present Al^{3+}-doped $Y_{(0.95-x)}Eu_{0.05}PO_4$ phosphor is similar to that found in most of the commercial phosphate laser glasses [22]. The observed photoluminescence pattern of the present Al^{3+}-doped $Y_{(0.95-x)}Eu_{0.05}PO_4$ powder phosphors is found similar to that reported in case of $Y_{0.95}Eu_{0.05}PO_4$ samples [8, 23].

4 CONCLUSIONS

Different concentrations of Li/Al-doped YPO_4:$Eu_{0.05}$ phosphors have been prepared by the conventional solid state reaction method and are characterized by X-ray diffraction, scanning electron microscopy, excitation and emission measurements. The dependence of various optical and morphological properties of the prepared materials on Li/Al concentration has been discussed. Incorporation of Li^{+} and Al^{3+} ions into the YPO_4:Eu phosphors has enhanced the crystallinity, particle size and hence the luminescence properties. The optimum concentration in case of both Li and Al dopants are found to be 10 mol %. The improvement in PL performance with Li/Al-doping may result from the improved crystallinity and from the enlarged grain sizes inducing lower scattering loss and distortion of symmetry. The improvement of PL intensity with Li-doping may also result from formation of oxygen vacancies which act as sensitizers for energy transfer from host to Eu^{3+} ions. The results are discussed in comparison of results with similar reported works.

5 ACKNOWLEDGMENTS

This work was supported by Korea Research Foundation grant funded by the Korean Government (KRF-2007-412-J00902).

REFERENCES

[1] Z-J. Zhang, J-L. Yuan, S. Chen, H-H. Chen, X-X. Yang, J-T. Zhao, G-B. Zhang, C-S. Shi, Opt. Mater. 30 (2008) 1848.
[2] R. Balakrishnaiah, D. W. Kim, S. S. Yi, K. Jang, H. S. Lee, J. H. Jeong, Mater. Lett. 63 (2009) 2063.
[3] L. Sun, C. Qian, C. Liao, X. Wang, C. Yan, Solid State Commun. 119 (2001) 393.
[4] H. Lai, A. Bao, Y. Yang, Y. Tao, H. Yang, J. Nanopart. Res. 10 (2008) 1355.
[5] W. Di, X. Wang, B. Chen, H. Lai, X. Zhao, Opt. Mater. 27 (2005) 1386.
[6] R. S. Meltzer, S. P. Feofilov, J. Lumin. 102-3 (2003) 151.
[7] O. Guillot-Noel, B. Vianna, B. Bellamy, Opt. Mater. 13 (2000) 427.
[8] W. Di, X. Zhao, S. Lu, X. Wang, H. Zhao, J. Solid State Chem. 180 (2007) 2478.
[9] B. E. Warren, X-ray Diffraction, p. 253, Dover, New York, 1990.
[10] Y. Tao, G. Zhao, X. Ju, X. Shao, W. Zhang, S. Xia, Mater. Lett. 28 (1996) 17.
[11] Z. G. Wei, L. D. Sun, C. S. Liao, J. L. Yin, X. C. Jiang, C. H. Yan, J. Phys. Chem. B 106 (2002) 10610.
[12] J. H. Jeong, H. K. Yang, K. S. Shim, Y. R. Jeong, B. K. Moon, B. C. Choi, J. S. Bae, S. S. Yi, J. H. Kim, Appl. Surf. Sci. 253 (2007) 8273.
[13] S. S. Yi, J. S. Bae, K. S. Shim, J. H. Jeong, J. C. Park, P. H. Holloway, Appl. Phys. Lett. 84 (2004) 353.
[14] M. G. Hipolito, E. Martinez, O. A. Fregoso, C. Falcony, M. A. A. Frutis, J. Mater. Sci. Lett. 20 (2001) 1799.
[15] Q. Ma, Y. Zhou, A. Zhang, M. Lu, G. Zhou, C. Li, Solid State Sci. 11 (2009) 1124, and references there in.
[16] J. S. Bae, S. B. Kim, J. H. Jeong, J-C. Park, D-K. Kim, S-H. Byeon, S. S. Yi, Thin Solid Films 471 (2005) 224.
[17] J. S. Bae, S.S. Park, T. E. Hong, J. P. Kim, J. H. Yoon, E. D. Jeong, M. S. Won, J. H. Jeong, Curr. Appl. Phys. 9 (2009) S241.
[18] S. S. Yi, J. S. Bae, B. K. Moon, J. H. Jeong, J. C. Park, I. L. Kim, Appl. Phys. Lett. 81 (2002) 3344.
[19] L. Qiong, S. Yiguo, Y. Hongsheng, H. Wei, J. Rare Earths 26 (2008) 495.
[20] R. Brow, J. Am. Ceram. Soc. 76 (1993) 913.
[21] R. Brow, R. Kirkpatrick, G. Turner, J. Am. Ceram. Soc. 76 (1993) 919.
[22] J. H. Campbell, T. I. Suratwala, J. Non-Cryst. Solids 263&264 (2000) 318.
[23] Z. Cuihong, Z. Weichang, W. Lu, Rare Metals 27 (2008) 354.